Electronic Supplementary Material (ESI) for Sustainable Energy & Fuels.

Supplementary information

Impact of Lifetime on the Levelized Cost of Electricity from Perovskite Single Junction and Tandem Solar Cells

Ramez Hosseinian Ahangharnejhad,[1] Adam B. Phillips,[1] Zhaoning Song,[1] Ilke Celik,[2] Kiran Ghimire,[1] Prakash Koirala,[1] Randy J. Ellingson,[1] Robert W. Collins,[1] Nikolas J. Podraza,[1] Yanfa Yan,[1] and Michael J. Heben[1]

[1] *University of Toledo, Wright Center for Photovoltaics Innovation and Commercialization, Department of Physics and Astronomy, 2801 W. Bancroft St., Toledo, OH, 43606*

[2] *South Dakota School of Mines and Technology, Department of Civil and Environmental Engineering, 501 E. St. Joseph St., Rapid City, SD, 57701*

Methods

Annual energy yield (AEY)

The annual energy yield (AEY) results are given in table S1. The simulation method is the same as in our previous work.[1–3] Briefly, quantum efficiency (QE) is determined for the device structures shown in Figure 1, for angle of incident of solar irradiance for every hour of the year in Phoenix AZ. The QE calculations use the refractive indices for all the material in the thin film stack to calculate the absorption in each layer as well as the transmission and reflection at each interface. refractive index data for ITO and NiO were taken from ref. [4] and [5] respectively, while, refractive index for wide bandgap perovskite ($Cs_{0.05}FA_{0.8}MA_{0.15}PbI_{2.55}Br_{0.45}$)[6] and $MAPbI_3$, $Cu(In_{0.767}Ga_{0.233})Se_2$, CdS, Mo and ZnO were measured via ellipsometry.[7] The AEY model takes into account the impact of

Device Configuration	AEY in Phoenix AZ (kWh/m^2)
Two-terminal	533.90
Four-terminal	569.67
Perovskite	405.38
CIGS	393.59

Table. S1. Annual energy yield for different technologies calculated for Phoenix AZ.

temperatures, real world irradiances, anisotropy in power distribution of diffuse horizontal irradiance and the angles of incident throughout every hour of a year.

Manufacturing steps

The manufacturing costs (MC) for all the layers were taken from our previous contribution[8] except for the Mo, CIGS and CIGS buffer deposition which were taken from elsewhere.[9] The detailed costs and the steps are given in tables S2, S3, S4 and S5 for the two-terminal (2T), four-terminal (4T), and single junction CIGS and perovskite (PK), respectively.

Cost analysis for the LCOE analysis

The initial cost component for LCOE calculations for each PV configuration is determined as the sum of installation cost and the module cost. The module cost, or minimum

Step #	Steps	Deprecation $/m2	Maintenance $/m2	Utility $/m2	Labor $/m2	Material $/m2	Total $/m2
1	Back glass	0.158	0.011	0.259	0.231	3.037	3.696
2	Mo deposition	1.24	0.35	0.45	0.21	1.96	4.21
3	Laser scribe	0.191	0.019	0.008	0.009		0.227
4	CIGS deposition	6.42	1.68	0.38	0.27	3.9	12.65
5	CdS deposition	1.78	0.46	0.65	0.21	2.07	5.17
6	ITO deposition	0.9	0.232	0.394	0.116	1.298	2.94
7	NiO print	0.203	0.023	0.066	0.27	0.143	0.705
8	Perovskite print	0.236	0.032	0.062	0.502	0.222	1.054
9	ZnO print	0.223	0.023	0.058	0.077	0.059	0.44
10	Laser scribe	0.191	0.019	0.008	0.009		0.227
11	ITO deposition	0.9	0.232	0.394	0.116	1.298	2.94
12	Laser scribe	0.191	0.019	0.008	0.009		0.227
13	Interconnection	0.2	0.023	0.008	0.019	0.011	0.261
14	Edge seal	0.181	0.017	0.002	0.019	3.888	4.107
15	Lamination	0.19	0.02	0.028	0.077	1.535	1.85
16	Front glass	0.158	0.011	0.259	0.231	7	7.659
17	Junction box	0.158	0.01	0.002	0.019	7.5	7.689
		13.52	3.181	3.036	2.394	33.764	56.052

Table S2. Two-terminal tandem module manufacturing cost breakdown

sustainable price (MSP) for a given module configuration manufacturer is determined as the minimum selling price at which the internal rate of return (IRR) for the PV manufacturer is equal to the weighted average cost of capital (WACC) following

$$MSP = MC + OH + WACC$$

where OH is the overhead cost and is comprised of sales, general, and administrative (SG&A); research and development (R&D), taxes & interest. Details of these are given in table S7.

Step #	Steps	Deprecation $/m2	Maintenance $/m2	Utility $/m2	Labor $/m2	Material $/m2	Total $/m2
1	Back glass	0.158	0.011	0.259	0.231	3.037	3.696
2	Mo deposition	1.24	0.35	0.45	0.21	1.96	4.21
3	Laser scribe	0.191	0.019	0.008	0.009		0.227
4	CIGS deposition	6.42	1.68	0.38	0.27	3.9	12.65
5	CdS deposition	1.78	0.46	0.65	0.21	2.07	5.17
6	Laser scribe	0.191	0.019	0.008	0.009		0.227
7	ITO deposition	0.9	0.232	0.394	0.116	1.298	2.94
8	Laser scribe	0.191	0.019	0.008	0.009		0.227
9	Front glass	0.158	0.011	0.259	0.231	7	7.659
10	ITO deposition	0.9	0.232	0.394	0.116	1.298	2.94
11	Laser scribe	0.191	0.019	0.008	0.009		0.227
12	NiO print	0.203	0.023	0.066	0.27	0.143	0.705
13	Perovskite print	0.236	0.032	0.062	0.502	0.222	1.054
14	ZnO print	0.223	0.023	0.058	0.077	0.059	0.44
15	Laser scribe	0.191	0.019	0.008	0.009		0.227
16	ITO deposition	0.9	0.232	0.394	0.116	1.298	2.94
17	Laser scribe	0.191	0.019	0.008	0.009		0.227
18	Interconnection	0.2	0.023	0.008	0.019	0.011	0.261
19	Edge seal	0.181	0.017	0.002	0.019	3.888	4.107
20	Lamination	0.19	0.02	0.028	0.077	1.535	1.85
21	Junction box	0.158	0.01	0.002	0.019	7.5	7.689
22	Junction box	0.158	0.01	0.002	0.019	7.5	7.689
		15.151	3.48	3.456	2.556	42.562	67.362

Table S3. Four-terminal perovskite/CIGS tandem module manufacturing cost breakdown

Step #	Steps	Deprecation ($/m^2)	Maintenance ($/m^2)	Utility ($/m^2)	Labor ($/m^2)	Material ($/m^2)	Total ($/m^2)
1	Back glass	0.158	0.011	0.259	0.231	3.037	3.696
2	Mo deposition	1.24	0.35	0.45	0.21	1.96	4.21
3	Laser scribe	0.191	0.019	0.008	0.009		0.227
4	CIGS deposition	6.42	1.68	0.38	0.27	3.9	12.65
5	CdS deposition	1.78	0.46	0.65	0.21	2.07	5.17
6	Laser scribe	0.191	0.019	0.008	0.009		0.227
7	ITO deposition	0.9	0.232	0.394	0.116	1.298	2.94
8	Laser scribe	0.191	0.019	0.008	0.009		0.227
9	Interconnection	0.2	0.023	0.008	0.019	0.011	0.261
10	Edge seal	0.181	0.017	0.002	0.019	3.888	4.107
11	Lamination	0.19	0.02	0.028	0.077	1.535	1.85
12	Front glass	0.158	0.011	0.259	0.231	7	7.659
13	Junction box	0.158	0.01	0.002	0.019	7.5	7.689
		11.958	2.871	2.456	1.429	32.199	50.913

Table S4. CIGS module manufacturing cost breakdown

Step #	Steps	Deprecation ($/m^2)	Maintenance ($/m^2)	Utility ($/m^2)	Labor ($/m^2)	Material ($/m^2)	Total ($/m^2)
1	Front glass	0.158	0.011	0.259	0.231	7	7.659
2	ITO deposition	0.9	0.232	0.394	0.116	1.298	2.94
3	Laser scribe	0.191	0.019	0.008	0.009		0.227
4	NiO Print	0.203	0.023	0.066	0.27	0.143	0.705
5	Perovskite print	0.236	0.032	0.062	0.502	0.222	1.054
6	ZnO print	0.223	0.023	0.058	0.077	0.059	0.44
7	Laser scribe	0.191	0.019	0.008	0.009		0.227
8	Al deposition	0.9	0.232	0.394	0.116	1.298	2.94
9	Laser scribe	0.191	0.019	0.008	0.009		0.227
10	Interconnection	0.2	0.023	0.008	0.019	0.011	0.261
11	Edge seal	0.181	0.017	0.002	0.019	3.888	4.107
12	Lamination	0.19	0.02	0.028	0.077	1.535	1.85
13	Back glass	0.158	0.011	0.259	0.231	3.037	3.696
14	Junction box	0.158	0.01	0.002	0.019	7.5	7.689
		4.08	0.691	1.556	1.704	25.834	34.022

Table S5. Perovskite module manufacturing cost breakdown

T85 (year)	Degradation rate *d* (%)
1	15.00
2	7.80
3	5.27
4	3.98
5	3.20
6	2.67
7	2.29
8	2.01
9	1.79
10	1.61
11	1.47
12	1.35
13	1.24
14	1.15
15	1.08
16	1.01
17	0.95
18	0.90
19	0.85
20	0.81
21	0.77
22	0.74
23	0.70
24	0.67
25	0.65
26	0.62
27	0.60
28	0.58
29	0.56
30	0.54

Table S6. Lifetime and corresponding degradation rate.

Financial parameters	
Real discount rate	6.5% [10]
WACC	14% [10]
Inflation rate	2.5% [11]
Effective tax rate	27% [9]
R&D	2.5% [9]
SG&A	8.5% [9]

Table S7. Financial parameters used for the MSP and LCOE calculation.

The installation costs are taken from the NREL benchmark. Note that there are area (eg., electrical and structural BOS) and power (eg., inverter) dependent costs in this analysis. We convert all values to power dependent costs using the plant size.

NREL 2018 benchmark installation costs:

- Inverter: 0.04 \$/W[12]
- Other installation costs (electrical, structural BOS, labor): 0.55 \$/W[12]
- O&M: 13 \$/kWh[12]
- 100MW plant size: 523,560 $m^2 \simeq 0.525$ km^2

4T incremental cost:

Table S8 shows the additional costs for the 4T tandem assumed in this work. The LCOE analysis with the low additional cost is shown in figure 2. The LCOE results for 4T with medium and high additional costs are given in figure S1(a) and (b) respectively. As with

	Low additional cost for 4T	**Medium additional cost for 4T**	**High additional cost for 4T**
Inverter	+ 0.01 \$/W	+ 0.02 \$/W	+0.04\$/W
Other installation costs	+ 0.03 \$/W	+ 0.06 \$/W	+ 0.12 \$/W
O&M	+ 2 \$/kWh	+ 4 \$/kWh	+ 6 \$/kWh

Table S8. Assumed additional costs of installation and O&M considered for the 4T tandems.

the low additional cost, in figure 2(e), 4T does not appear in the LCOE phase diagram plot of the module types with lowest LCOE for medium and high additional costs of 4T. The LCOE of 4T as function of perovskite T85 and deployment time with no additional cost of installation is shown in figure S1(c). For no additional cost for 4T installation, the 4T appears in the lowest LCOE phase diagram plot. The lowest LCOE plot with no additional cost of installation of 4T is shown in figure S1(d).

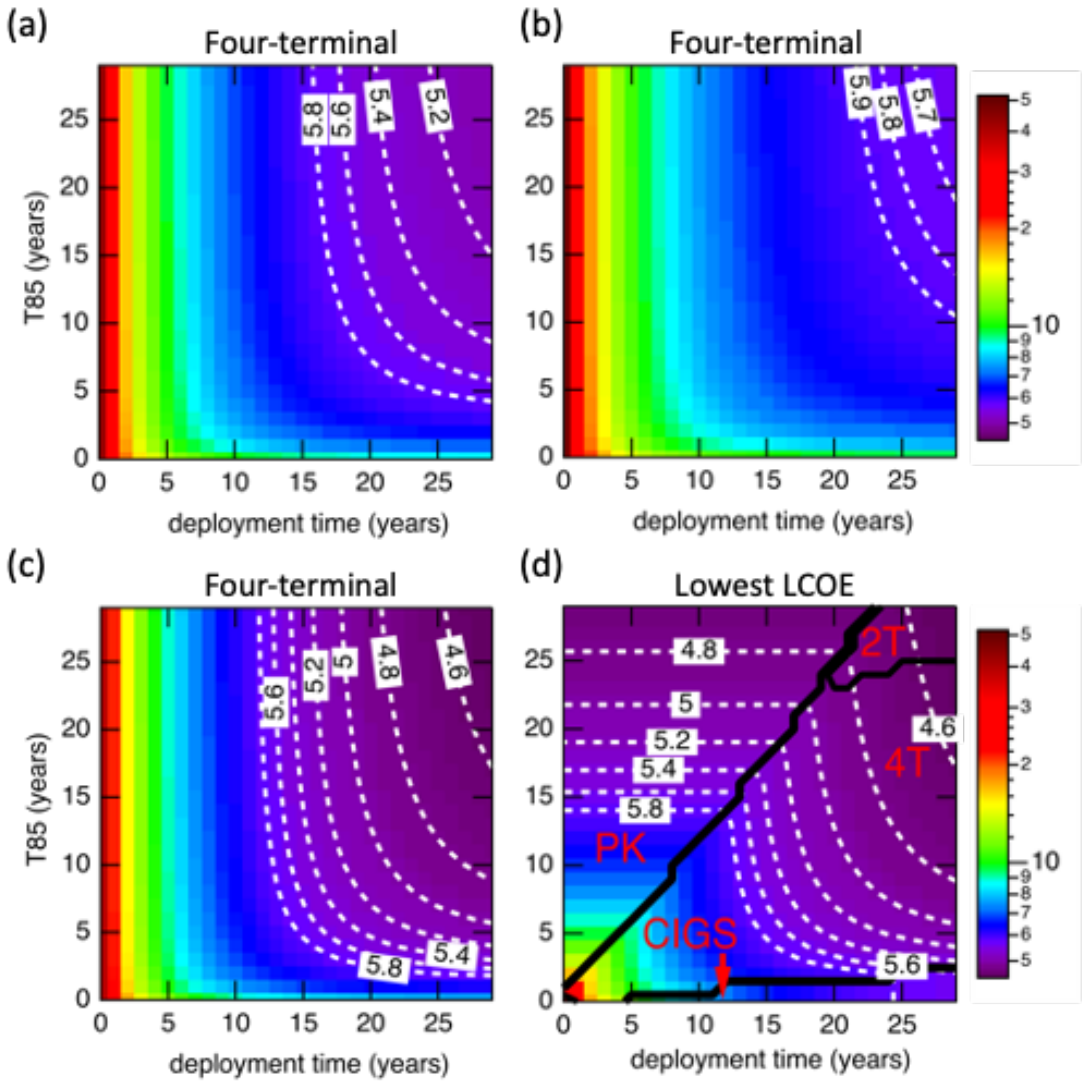

Figure S1. LCOE of 4T tandem as function of perovskite T85 and deployment time for (a) medium (b) high and (c) no additional costs of installation and O&M. (d) Lowest LCOE as function of perovskite T85 and deployment time for 4T tandem without any additional cost of installation and 2T subcells degrading with MPP loss is shown.

2T degradation modes:

Three different degradation modes were explored for 2T tandems. The difference among these modes were in the top perovskite cell degradation which were assumed to be loss in short circuit current, open circuit voltage and maximum power point (MPP) while the degradation at the bottom cell was assumed to be in MPP. To determine the degradation rate as function of perovskite T85 and deployment time for each of these degradation modes, the PCE of 2T tandem was determined from the tandem JV curve. The tandem JV curve is calculated using method described elsewhere.[13] The degraded subcell JV curve was determined by scaling down the corresponding parameter (current, voltage or MPP) by a degradation ratio:

$$degradation\ ratio_{PK} = (1 - d_{PK})^{deployment\ time}$$

$$degradation\ ratio_{CIGS} = (1 - d_{CIGS})^{deployment\ time}$$

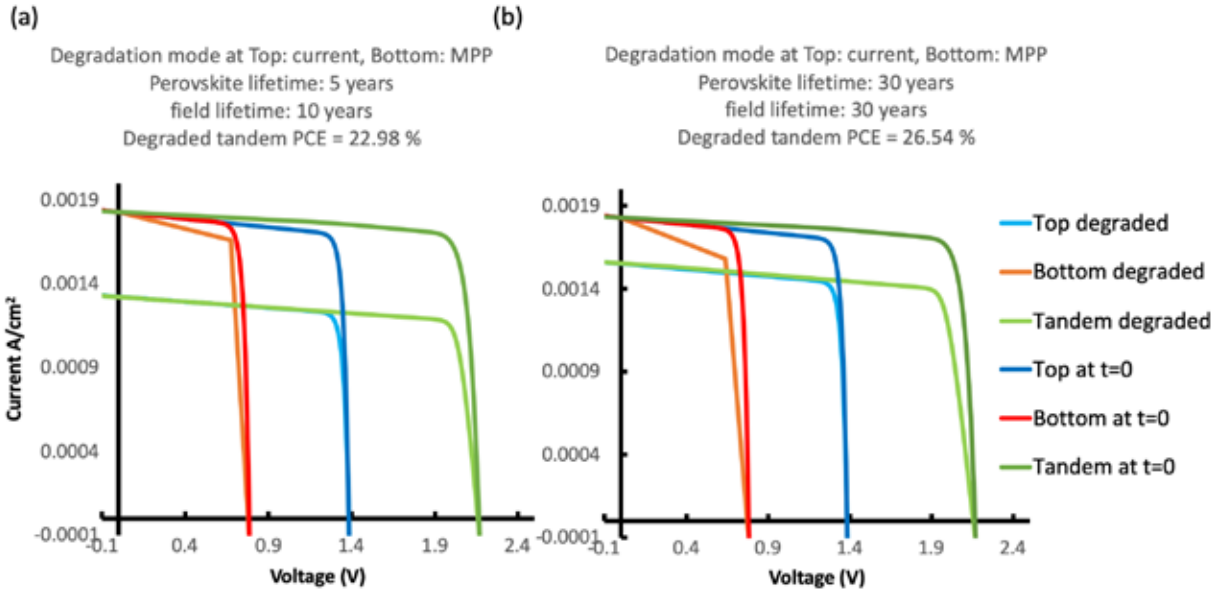

Figure S2. JV curves of subcells and 2T tandem at t=0 and degraded with PK T85 and deployment time of (a) 5 and 10 years, respectively, and (b) 30 and 30 years, respectively. The degradation of the top cell is loss in current. The degraded 2T tandem PCE is shown for each panel.

where d_{PK} is the degradation rate for PK subcell and is determined using equation 2 and is based on the PK T85 (table S6) and d_{CIGS} is the degradation rate for the CIGS subcell and is assumed to be 0.54% annually corresponding to 30 year T85 lifetime. For MPP degradation mode, both current and voltage at MPP are scaled down by the square root of the ratio and the JV curve is interpolated from the MPP to Voc and Jsc points. Figure S2 shows the subcell and tandem JV curves for device at t=0 and degraded ones for (a) 5 year PK T85 and 10 year deployment time and (b) 30 year PK T85 and 30 year deployment time with current loss as degradation mode at the top perovskite subcell. Figures S3 and S4 show the same for the MPP and voltage loss as degradation mode of the perovskite subcell respectively. Note that smoothing of the MPP degraded JV curves can lead to more realistic curves, but has little effect on the LCOE calculation.

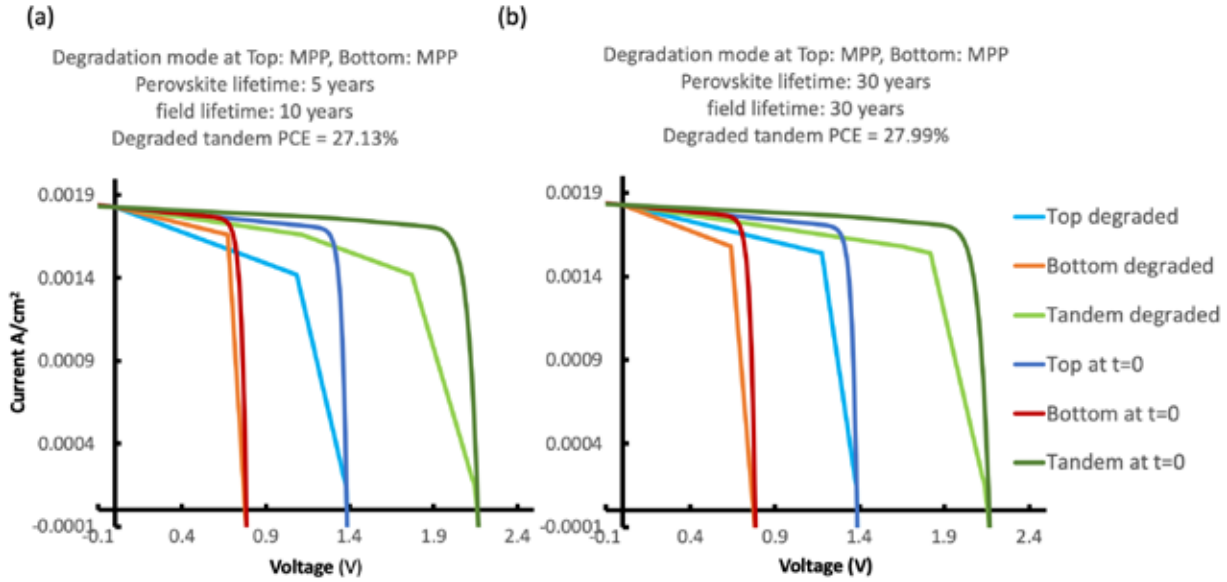

Figure S3. JV curves of subcells and 2T tandem at t=0 and degraded with PK T85 and deployment time of (a) 5 and 10 years, respectively, and (b) 30 and 30 years, respectively. The degradation of the top cell is loss in MPP. The degraded 2T tandem PCE is shown for each panel.

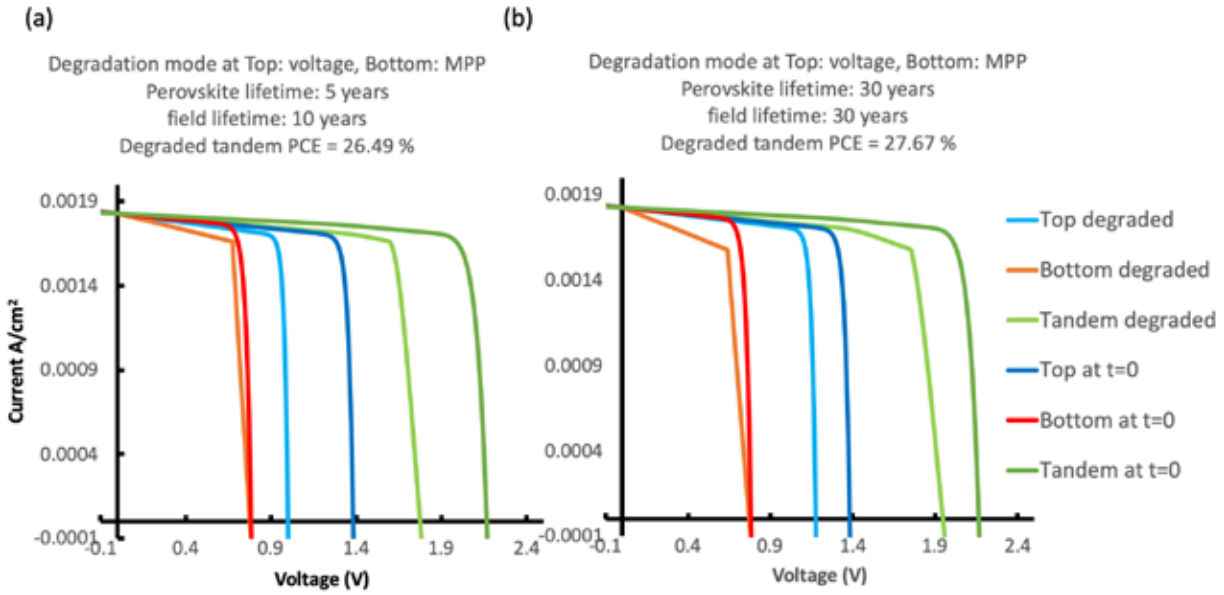

Figure S4. JV curves of subcells and 2T tandem at t=0 and degraded with PK T85 and deployment time of (a) 5 and 10 years, respectively, and (b) 30 and 30 years, respectively. The degradation of the top cell is loss in voltage. The degraded 2T tandem PCE is shown for each panel.

The degraded tandem PCE is shown for each case and the tandem degradation rate for the given PK T85 and deployment time is determined based on the PCE loss ratio from the PCE at t=0.

PCE of the degraded 2T tandems as function of top perovskite subcell T85 and deployment time for the top cell perovskite degradation modes of current, MPP and voltage loss are calculated and shown in figure S5, panels (a), (b) and (c) respectively. The resultant degradation modes were used to determine the LCOE of 2T tandem. The LCOE results for MPP loss as degradation mode of perovskite subcell is given in figure 2 (d). Figure S6 show the same for the current (a) and voltage (b) loss as degradation modes of the perovskite subcell.

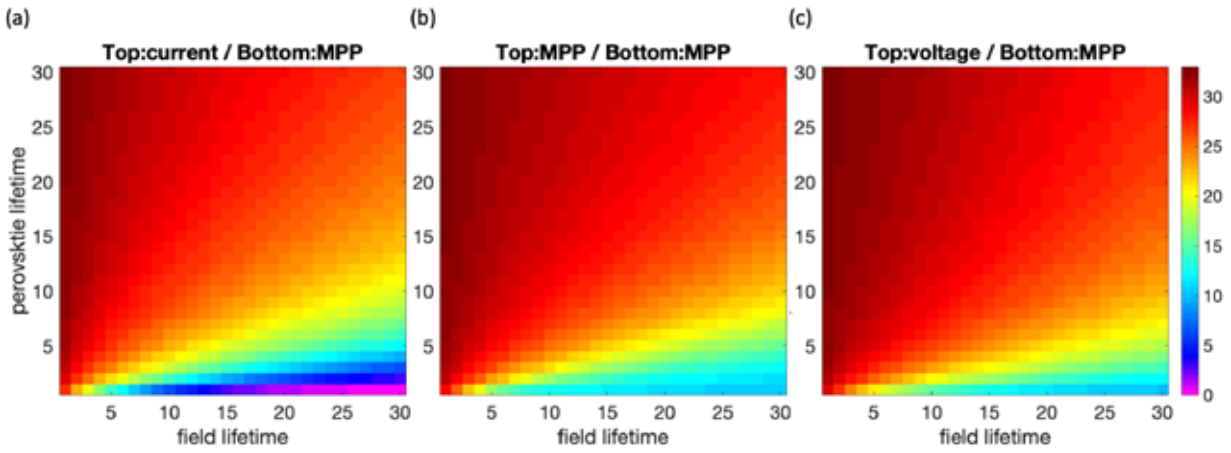

Figure S5. PCE of degraded 2T tandem as function of perovskite T85 and deployment time for (a) current, (b) MPP and (c) voltage loss as degradation mode at the top perovskite subcell. The bottom subcell degradation rate is assumed to be 0.54% annually and the degradation mode is MPP loss.

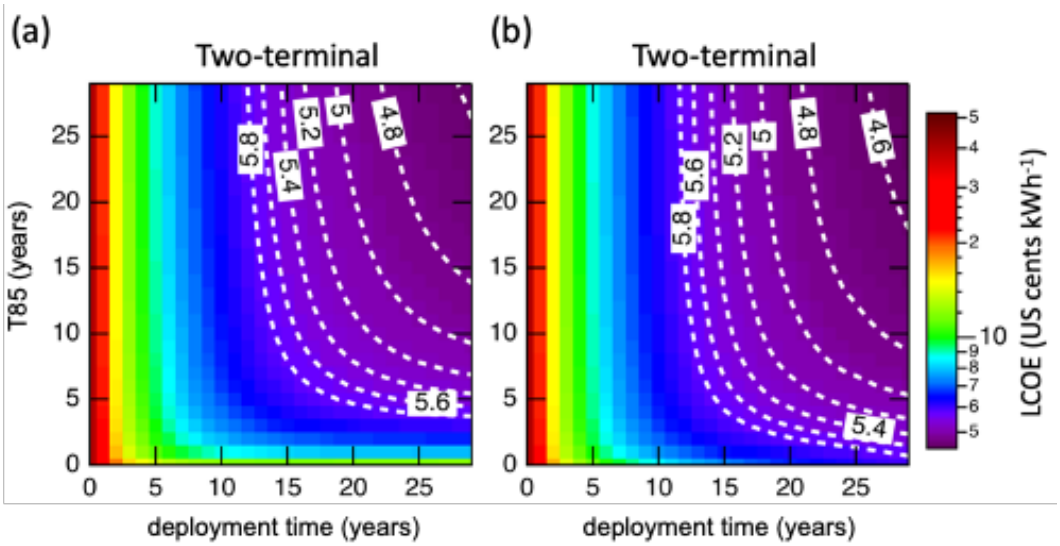

Figure S6. LCOE of 2T tandems as function of perovskite T85 and deployment time for degradation at (a) current and (b) voltage at the top subcell and the MPP degradation at the bottom subcell.

Bottom cell manufacturing cost

LCOE of CIGS in the single junction configuration as function of manufacturing cost is given in figure S7(a). Figure S7(b) and (c) shows the LCOE of 2T and 4T as function of CIGS manufacturing cost and perovskite T85.

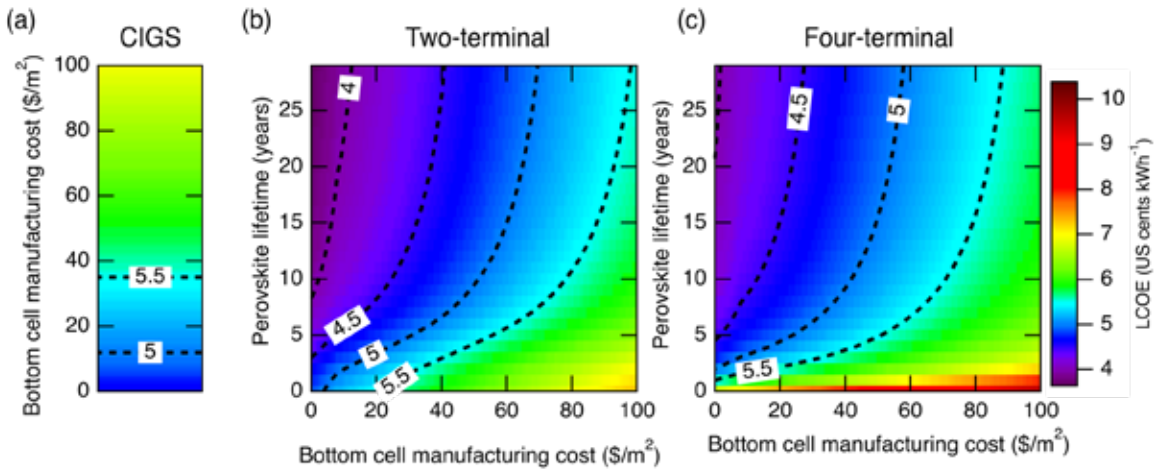

Figure S7. LCOE of (a) CIGS, (b) 2T and (c) 4T as function of CIGS manufacturing cost and PK T85.

Reference

1 R. Hosseinian Ahangharnejhad, A. B. Phillips, K. Ghimire, P. Koirala, Z. Song, H. M. Barudi, A. Habte, M. Sengupta, R. J. Ellingson, Y. Yan, R. W. Collins, N. J. Podraza and M. J. Heben, *Sustain. Energy Fuels*, 2019, **3**, 1841–1851.

2 R. Hosseinian Ahangharnejhad, Z. Song, A. B. Phillips, S. C. Watthage, Z. S. Almutawah, D. R. Sapkota, P. Koirala, R. W. Collins, Y. Yan and M. J. Heben, *MRS Adv.*, 2018, **3**, 3111–3119.

3 R. Hosseinian Ahangharnejhad, W. Becker, J. Jones, A. Anctil, Z. Song, A. Phillips, M. Heben and I. Celik, *Cell Reports Phys. Sci.*

4 T. A. F. Konig, P. A. Ledin, J. Kerszulis, M. A. Mahmoud, M. A. El-sayed, J. R. Reynolds and V. V Tsukruk, *ACS Nano*, 2014, **8**, 6182–6192.

5 J. W. Shim, C. Fuentes-Hernandez, A. Dindar, Y. Zhou, T. M. Khan and B. Kippelen, *Org. Electron.*, 2013, **14**, 2802–2808.

6 Z. Song, D. Zhao, C. Chen, C. L. Ramez H Ahangharnejhad, K. Ghimire, N. J. Podraza, M. J. Heben, K. Zhu and Y. Yan, in *2019 IEEE 46th Photovoltaic Specialists Conference (PVSC)*, 2019, pp. 0743–0746.

7 A. R. A. Ibdah, P. Koirala, P. Aryal, P. Pradhan, M. J. Heben, N. J. Podraza, S. Marsillac and R. W. Collins, *J. Energy Chem.*, 2017, **27**, 1151–1169.

8 Z. Song, C. L. McElvany, A. B. Phillips, I. Celik, P. W. Krantz, S. C. Watthage, G. K. Liyanage, D. Apul and M. J. Heben, *Energy Environ. Sci.*, 2017, **10**, 1297–1305.

9 S. E. Sofia, J. P. Mailoa, D. N. Weiss, B. J. Stanbery, T. Buonassisi and I. M. Peters, *Nat. Energy*, 2018, **3**, 387–394.

10 D. Feldman, T. Lowder and P. Schwabe, *PV Project Finance in the United States*, 2016.

11 R. Jones-Albertus, D. Feldman, R. Fu, K. Horowitz and M. Woodhouse, *Prog. Photovoltaics*, 2016, **24**, 1272–1283.

12 R. Fu, D. Feldman and R. Margolis, *U.S. Solar Photovoltaic System Cost Benchmark: Q1 2018*, 2018.

13 A. Hadipour, B. de Boer and P. W. M. Blom, *Org. Electron. physics, Mater. Appl.*, 2008, **9**, 617–624.